Lieb-Liniger Bosons in a Shallow Quasiperiodic Potential: Bose Glass Phase and Fractal Mott Lobes

Yao, Hepeng; Giamarchi, Thierry; Sanchez-Palencia, Laurent

How to cite

YAO, Hepeng, GIAMARCHI, Thierry, SANCHEZ-PALENCIA, Laurent. Lieb-Liniger Bosons in a Shallow Quasiperiodic Potential: Bose Glass Phase and Fractal Mott Lobes. In: Physical Review Letters, 2020, vol. 125, n° 060401. doi: 10.1103/PhysRevLett.125.060401

This publication URL: https://archive-ouverte.unige.ch/unige:147108
Publication DOI: 10.1103/PhysRevLett.125.060401

Lieb-Liniger Bosons in a Shallow Quasiperiodic Potential: Bose Glass Phase and Fractal Mott Lobes

Hepeng Yao,[1] Thierry Giamarchi,[2] and Laurent Sanchez-Palencia[1]
[1]CPHT, CNRS, Institut Polytechnique de Paris, Route de Saclay 91128 Palaiseau, France
[2]Department of Quantum Matter Physics, University of Geneva, 24 Quai Ernest-Ansermet, CH-1211 Geneva, Switzerland

(Received 16 February 2020; accepted 13 July 2020; published 3 August 2020)

The emergence of a compressible insulator phase, known as the Bose glass, is characteristic of the interplay of interactions and disorder in correlated Bose fluids. While widely studied in tight-binding models, its observation remains elusive owing to stringent temperature effects. Here we show that this issue may be overcome by using Lieb-Liniger bosons in shallow quasiperiodic potentials. A Bose glass, surrounded by superfluid and Mott phases, is found above a critical potential and for finite interactions. At finite temperature, we show that the melting of the Mott lobes is characteristic of a fractal structure and find that the Bose glass is robust against thermal fluctuations up to temperatures accessible in quantum gases. Our results raise questions about the universality of the Bose glass transition in such shallow quasiperiodic potentials.

DOI: 10.1103/PhysRevLett.125.060401

The interplay of interactions and disorder in quantum fluids is at the origin of many intriguing phenomena, including many-body localization [1–5], collective Anderson localization [6–13], and the emergence of new quantum phases. For instance, a compressible insulator, known as the Bose glass (BG) [14–18], may be stabilized against the superfluid (SF) and, in lattice models, against the Mott insulator (MI). One-dimensional (1D) systems are particularly fascinating for the SF may be destabilized by arbitrary weak perturbations, an example of which is the pinning transition in periodic potentials [19–23]. Similarly, above an interaction threshold, the BG transition can be induced by arbitrary weak disorder [14,15]. The phase diagram of 1D disordered bosons has been extensively studied and is now well characterized theoretically [17,18,24–27]. The experimental observation of the BG phase remains, however, elusive [28–33], despite recent progress using ultracold atoms in quasiperiodic potentials [34,35].

Controlled quasiperiodic potentials, as realized in ultracold atom [36–38] and photonic [39–42] systems, have long been recognized as a promising alternative to observe the BG phase. So far, however, this problem has been considered only in the tight-binding limit, known as the Aubry-André model [43–47]. It sets the energy scale to the tunneling energy, which is exponentially small in the main lattice amplitude and of the order of magnitude of the temperature in typical experiments. The phase coherence is then strongly reduced, which significantly alters the phase diagram. Although such systems give some evidence of a Bose glass phase [34,35], they require a heavy heuristic analysis of the data to factor out the very important effects of the temperature.

Here, we propose to overcome this issue by using shallow quasiperiodic potentials. The energy scale would then be the recoil energy, which is much larger than typical temperatures in ultracold-atom experiments [36,48]. This, however, raises the fundamental question of whether a BG phase can be stabilized in this regime: In the hard-core limit, interacting bosons map onto free fermions [49]. A band of localized (resp. extended) single particles then maps onto the BG (resp. SF) phase while a band gap maps onto the MI phase. In the shallow bichromatic lattice, however, it has been shown that band gaps, i.e., MI phases, are dense [50] and the BG would thus be singular. On the other hand, decreasing the interactions down to the mean field regime favors the SF phase [14,15,25,51]. Hence, a BG can only be stabilized, if at all, for intermediate interactions.

We tackle this issue using exact quantum Monte Carlo (QMC) calculations. We compute the exact phase diagram of interacting bosons in a shallow 1D bichromatic lattice. Our results are summarized in Fig. 1. Our main finding is that, at zero temperature, a significant BG phase can be stabilized above a critical quasiperiodic amplitude and for intermediate interaction strengths (see upper row on Fig. 1). Further, we study the melting of the quantum phases at finite temperature. We show that their main features are robust against thermal fluctuations up to temperatures accessible to experiments, in spite of the growth of a normal fluid (NF) regime (see lower row in Fig. 1). Moreover, while the SF and BG phases progressively cross over to the NF regime, we find that the MI phase shows a transient anomalous temperature-induced enhancement of coherence. We show that the melting of

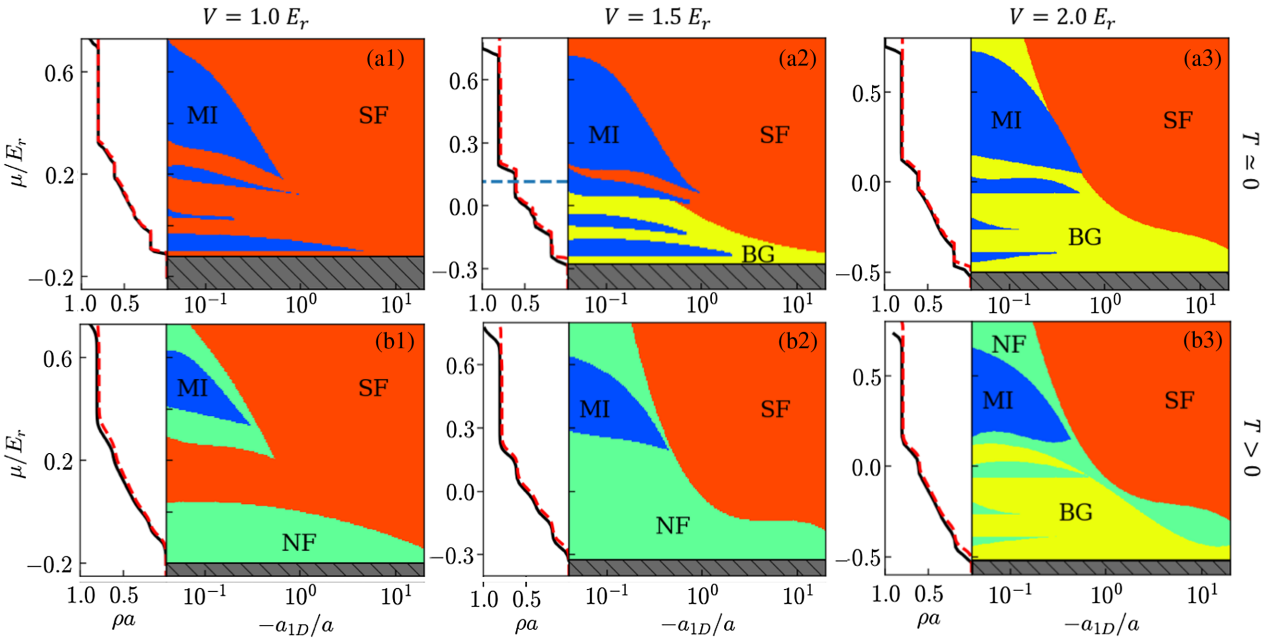

FIG. 1. Phase diagrams of Lieb-Liniger bosons in a shallow quasiperiodic potential for increasing values of the potential ($V = E_r < V_c$, $V = 1.5E_r \gtrsim V_c$, and $V = 2E_r > V_c$). Upper row: Quantum phase diagrams from QMC calculations at a vanishingly small temperature [$k_BT = 10^{-3}E_r$ for (a1) and $k_BT = 2 \times 10^{-3}E_r$ for (a2) and (a3)]. Lower row: Counterpart of the upper row at the finite temperature $k_BT = 0.015E_r$. On the left of each panel, we show the equation of state $\rho(\mu)$ at strong repulsive interactions, $-a_{1D}/a = 0.05$ (solid black line) together with that of free fermions at the corresponding temperatures (dashed red line). Note that the smallest band gaps are smoothed out by the finite temperatures [52]. The dotted blue line in (a2) shows the single-particle ME at $V = 1.5E_r$, $E_c \simeq 0.115E_r$.

the MI phase presents a characteristic algebraic temperature dependence, which we relate to the fractal structure of the MI lobes.

Model and approach.—The system we consider is a Lieb-Liniger gas, i.e., a 1D N-boson gas with repulsive contact interactions, subjected to a quasiperiodic potential $V(x)$. It is governed by the Hamiltonian

$$\mathcal{H} = \sum_{1\le j\le N}\left[-\frac{\hbar^2}{2m}\frac{\partial^2}{\partial x_j^2} + V(x_j)\right] + g\sum_{j<\ell}\delta(x_j - x_\ell), \quad (1)$$

where m is the particle mass, x the space coordinate, $g = -2\hbar^2/ma_{1D}$ the coupling constant, and $a_{1D} < 0$ the 1D scattering length (corresponding to repulsive interactions [60]). The quasiperiodic potential is bichromatic with equal amplitudes, i.e.,

$$V(x) = \frac{V}{2}[\cos(2k_1x) + \cos(2k_2x + \varphi)], \quad (2)$$

with incommensurate spatial frequencies k_1 and k_2, and we used $\varphi = 0.2$. Qualitatively similar results are expected for imbalanced potentials and different incommensurate ratios $r = k_2/k_1$, although the value of the critical localization potential may vary [50,53]. In this respect, the balanced case is nearly optimal [50] and we choose $r \simeq 0.807$, close to the experiments of Refs. [34,35,61]. In the following, we use the spatial period of the first lattice, $a = \pi/k_1$, and the corresponding recoil energy, $E_r = \hbar^2k_1^2/2m$, as the space and energy units, respectively. Using these units, typical interaction and temperature ranges in recent experiments are $-a_{1D}/a \simeq 0.06$–20 and $k_BT/E_r \simeq 0.015$–0.15 [22,23,34,54].

Let us start with the single-particle problem, which is relevant to the hard-core limit. The localization and spectral properties of single particles in the shallow bichromatic lattice Eq. (2) have been studied previously [50,53,62,63]. Below some critical amplitude $V_c \sim E_r$, all the states are extended, while above V_c, a band of localized states appears at low energy, up to an energy mobility edge (ME) E_c. The existence of a finite E_c distinguishes the shallow lattice model from the celebrated Aubry-André tight-binding model, where it is absent. We determine the single-particle eigenstates using exact diagonalization and the critical amplitude is precisely found from the finite-size scaling analysis of their inverse participation ratio. We then find $V_c/E_r \simeq 1.38 \pm 0.01$ [52].

Phase diagrams for interacting bosons.—We now turn to the interacting Lieb-Liniger gas. At zero temperature, we expect three possible phases: the MI (incompressible insulator), the SF (compressible superfluid), and the BG (compressible insulator). They are identified through the values of the compressibility κ and the superfluid fraction f_s. We have also checked that the one-body correlation function $g_1(x) =$

$\int (dx'/L)\langle \Psi(x'+x)^\dagger \Psi(x')\rangle$ decays exponentially in the insulating phases (MI and BG) and algebraically in the SF phase (see below). All these quantities are found using quantum Monte Carlo calculations in continuous space within the grand-canonical ensemble (temperature T and particle chemical potential μ) [52].

The upper row in Fig. 1 shows the quantum phase diagrams versus the inverse interaction strength and the chemical potential, for increasing amplitudes of the quasiperiodic potential. They are found from QMC calculations of κ and f_s at a vanishingly small temperature [52]. In practice, we have used $k_B T \sim 0.001$–$0.002 E_r$, where k_B is the Boltzmann constant, and we have checked that there is no sizable temperature dependence at a lower temperature. For $V < V_c$, no localization is expected and we only find SF and MI phases; see Fig. 1(a1). The SF dominates at large chemical potentials and weak interactions. Strong enough interactions destabilize the SF phase and Mott lobes open, with fractional occupation numbers ($\rho a = r$, $2r-1$, $2-2r$, $1-r$ from top to bottom). The number of lobes increases with the interaction strength and eventually become dense in the hard-core limit (see below). For $V > V_c$ and a finite interaction, a BG phase develops in between the MI lobes up to the single-particle ME at $\mu = E_c$; see Fig. 1(a2). There, the SF fraction is strictly zero and the compressibility has a sizable, nonzero value, within QMC accuracy. When the quasiperiodic amplitude V increases, the BG phase extends at the expense of both the MI and SF phases; see Fig. 1(a3).

The lower row in Fig. 1 shows the counterpart of the previous diagrams at the finite temperature $T = 0.015 E_r/k_B$, corresponding to the minimal temperature in Ref. [54]. While quantum phases may be destroyed by arbitrarily small thermal fluctuations, the finite-size systems we consider ($L = 83a$, of the order of typical sizes in experiments [28,31,34]) retain characteristic properties, reminiscent of the zero-temperature phases. The SF, MI, and BG *regimes* shown in Figs. 1(b1)–1(b3) are identified accordingly. While the former two are easily identified, special care should be taken for the BG, which cannot be distinguished from the normal fluid via κ and f_s, since both are compressible insulators. A key difference, however, is that correlations are suppressed by the disorder in the BG and by thermal fluctuations in the NF. To identify the BG regime, we thus further require that the suppression of correlations is dominated by the disorder; i.e., the correlation length is nearly independent of the temperature. The QMC results show that the NF develops at low density and strong interactions; see Fig. 1(b1). For a moderate quasiperiodic amplitude, it takes over the BG, which is completely destroyed; see Fig. 1(b2). For a strong enough quasiperiodic potential, however, the BG is robust against thermal fluctuations and competes favorably with the NF regime; see Fig. 1(b3). We hence find a sizable BG regime, which should thus be observable at temperatures accessible to current experiments using 1D quantum gases.

Melting of the quantum phases.—We now turn to the quantitative study of the temperature effects. We compute the one-body correlation function and fit it to $g_1(x) \sim \exp(-|x|/\xi)$, where ξ is the correlation length [52]. The typical behavior of $\xi(T)$ when increasing the temperature T from a point in the BG phase is displayed in Fig. 2(a) (black line). It shows a plateau at low temperature, which is identified as the BG regime. Above some melting temperature T^*, the thermal fluctuations suppress phase coherence and ξ decreases with T, as expected for a NF. In both the BG and NF regimes, superfluidity is absent and we consistently find $f_s = 0$, also shown in Fig. 2(a) (blue line).

Consider now increasing the temperature from a point in the SF phase at $T = 0$; see Fig. 2(b). For low enough T, we find a finite SF fraction f_s, which, however, strongly decreases with T. The sharp decrease of f_s allows us to identify a rather well-defined temperature T^* beyond which we find a NF regime, characterized by a vanishingly small f_s. We checked that, consistently, the correlation function turns at T^* from a characteristic algebraic to exponential decay over the full system of length $L = 83a$ [52].

Consider finally increasing the temperature from a point in a MI lobe at $T = 0$; see two typical cases in Figs. 2(c) and 2(d). As expected, below the melting temperature T^*, the correlation length shows a plateau, identified as the MI regime. Quite counterintuitively, however, we find that above T^* the phase coherence is enhanced by thermal fluctuations, up to some temperature T_m, beyond which it is finally suppressed. This anomalous behavior is signaled by the nonmonotony of the correlation length $\xi(T)$; see Fig. 2(c). In some cases, it is strong enough to induce

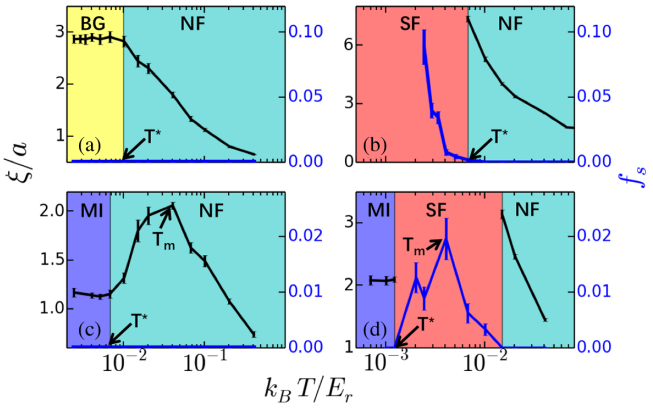

FIG. 2. Temperature-induced melting of the quantum phases. The various panels show the coherence length ξ (black lines) and the superfluid fraction f_s (blue lines) as a function of temperature for four typical cases. (a) BG to NF crossover ($V = 2E_r$, $\mu = -0.28E_r$, and $-a_{1D}/a = 4.0$), (b) SF to NF crossover ($V = 2E_r$, $\mu = 0.53E_r$, and $-a_{1D}/a = 0.2$), (c) MI to NF crossover ($V = 2E_r$, $\mu = 0.47E_r$, and $-a_{1D}/a = 0.2$), (d) MI to NF, via SF, crossover ($V = E_r$, $\mu = 0.2E_r$, and $-a_{1D}/a = 0.05$).

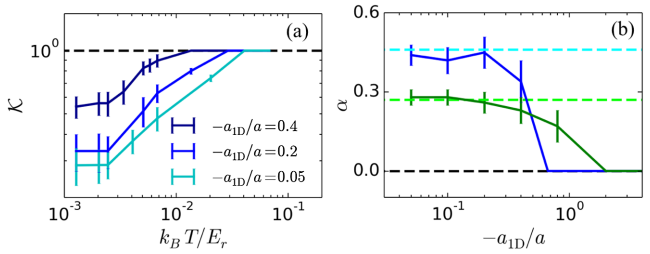

FIG. 3. Melting of the Mott phase. (a) Compressible phase fraction versus temperature for $V = 1.5E_r$, $\mu/E_r \in [-0.4, 0.8]$, and various interaction strengths. (b) Exponent α versus the interaction strength for $V = E_r$ (green solid line) and $V = 1.5E_r$ (blue). The colored dashed lines indicate the corresponding values of $1 - D_H$.

a finite superfluid fraction f_s, and correspondingly an algebraic correlation function in our finite-size system [52]; see Fig. 2(d). This is typically the case when the MI lobe is surrounded by a SF phase at $T = 0$. We interpret this behavior from the competition of two effects. On the one hand, a finite but small temperature permits the formation of particle-hole pair excitations, which are extended and support phase coherence. This effect, which is often negligible in strong lattices, is enhanced in shallow lattices owing to the smallness of the Mott gaps, particularly in the quasiperiodic lattice where Mott lobes with fractional fillings appear [45,50]. This favors the onset of a finite-range coherence at finite temperature. On the other hand, when the temperature increases, a larger number of extended pairs, which are mutually incoherent, is created. This suppresses phase coherence on a smaller and smaller length scale, hence competing with the former process and leading to the nonmonotonic temperature dependence of the coherence length.

Fractal Mott lobes.—The melting of a Mott lobe of gap Δ is expected at a temperature $T \propto \Delta/k_B$ [64]. In the quasiperiodic lattice, however, there is no typical gap, owing to the fractal structure of the Mott lobes, inherited from that of the single-particle spectrum [45,47,50]. To get further insight into the melting of the MI lobes, consider the compressible phase fraction, i.e., the complementary of the fraction of MI lobes,

$$\mathcal{K} = \lim_{q\to 0_+} \int_{\mu_1}^{\mu_2} \frac{d\mu}{\mu_2 - \mu_1} [\kappa(\mu)]^q, \tag{3}$$

in the chemical potential range $[\mu_1, \mu_2]$. The behavior of $\mathcal{K}$ versus temperature is shown in Fig. 3(a) for various interaction strengths. Below the melting temperature of the smallest MI lobes, $T_1^\star$, $\mathcal{K}$ is insensitive to thermal fluctuations and we correspondingly find $\mathcal{K} =$ constant. Above that of the largest lobe, $T_2^\star$, all MI lobes are melt and $\mathcal{K} = 1$ [65]. In the intermediate regime, $T_1^\star \lesssim T \lesssim T_2^\star$, we find the algebraic scaling $\mathcal{K} \sim T^\alpha$, where the exponent α depends on both the interaction strength and the quasiperiodic amplitude V; see Fig. 3(b). This behavior is reminiscent of the fractal structure of the MI lobes.

To understand this, consider the Tonks-Girardeau limit, $a_{1D} \to 0$, where the Lieb-Liniger gas may be mapped onto free fermions [49]. The particle density then reads as $\rho(\mu) \simeq (1/L)\sum_j f_{\rm FD}(E_j - \mu)$, where $f_{\rm FD}(E) = 1/(e^{E/k_BT} + 1)$ is the Fermi-Dirac distribution and E_j is the jth eigenenergy of the single-particle Hamiltonian. This picture provides a very good approximation of our QMC results at large interaction, irrespective of T and V; see left-hand panels of each plot in Fig. 1. The compressibility thus reads as $\kappa(\mu) \simeq (-1/L)\sum_j f'_{\rm FD}(E_j - \mu)$. Since $f'_{\rm FD} = \partial f_{\rm FD}/\partial E$ is a peaked function of typical width k_BT around the origin, we find

$$\kappa(\mu) \sim n_{\epsilon=k_BT}(\mu), \tag{4}$$

where $n_\epsilon(E)$ is the integrated density of states per unit length of the free Hamiltonian in the energy range $[E - \epsilon/2, E + \epsilon/2]$. Hence, the compressibility maps onto the integrated density of states, k_BT onto the energy resolution, and, up to the factor $k_BT/(\mu_2 - \mu_1)$, the compressible phase fraction onto the spectral box-counting number $N_B(\epsilon)$ introduced in Ref. [50]. We then find

$$\mathcal{K} \sim \frac{k_BT}{\mu_2 - \mu_1} N_B(\epsilon = k_BT) \sim T^{1-D_H}, \tag{5}$$

where D_H is the Hausdorff dimension of the free spectrum [52], and we recover the algebraic temperature dependence $\mathcal{K} \sim T^\alpha$, with $\alpha = 1 - D_H$.

To validate this picture, we have computed the exponent α by fitting curves as in Fig. 3(a) as a function of the interaction strength. The results are shown in Fig. 3(b) for two values of the quasiperiodic amplitude (colored solid lines). As expected, we find $\alpha \to 1 - D_H$ (colored dashed lines) in the Tonks-Girardeau limit, $a_{1D} \to 0$. When the interaction strength decreases, the fermionization picture breaks down. The exponent α then decreases and vanishes when the last MI lobe shrinks.

Moreover, our results show that the compressible BG fraction is suppressed at low temperature (since $\alpha > 0$) and strong interactions [see Fig. 3(a)]. This is consistent with the expected singularity of the BG phase in the hard-core limit, where the MI lobes become dense.

Conclusion.—In summary, we have computed the quantum phase diagram of Lieb-Liniger bosons in a shallow quasiperiodic potential. Our main result is that a BG phase emerges above a critical potential and for finite interactions, surrounded by SF and MI phases. We have also studied finite-temperature effects. We have shown that the melting of the MI lobes is characteristic of their fractal structure and found regimes where the BG phase is robust against thermal fluctuations up to a range accessible to experiments. This paves the way to the direct observation of the

still elusive BG phase, as well as the fractality of the MI lobes, in ultracold quantum gases.

More precisely, the temperature $T = 0.015E_r/k_B$ used in Fig. 1 corresponds to $T \simeq 1.5$ nK for ^{133}Cs ultracold atoms, which is about the minimal temperature achieved in Ref. [54]. Further, we have checked that a sizable BG regime is still observable at higher temperatures, for instance $T = 0.1E_r/k_B$ [52], which is higher than the temperatures reported in Refs. [34,54]. We propose to characterize the phase diagram using the one-body correlation function, as obtained from Fourier transforms of time-of-flight images in ultracold atoms [34,35]. Discrimination of algebraic and exponential decays could benefit from box-shaped potentials [66–68]. Our results indicate that the variation of the correlation length $\xi(T)$ with the temperature characterizes the various regimes; see Fig. 2.

Further, our work questions the universality of the BG transition found here. In contrast to truly disordered [14,15] or Fibonacci [69,70] potentials, the shallow bichromatic lattice contains only two spatial frequencies of finite amplitudes. Hence, the emergence of a BG requires the growth of a dense set of density harmonics within the renormalization group flow, which may significantly affect the value of the critical Luttinger parameter.

This research was supported by the European Commission FET-Proactive QUIC (H2020 Grant No. 641122), the Paris region DIM-SIRTEQ, and the Swiss National Science Foundation under Division II. This work was performed using HPC resources from GENCI-CINES (Grant No. 2018-A0050510300). Numerical calculations make use of the ALPS scheduler library and statistical analysis tools [71–73]. We thank the CPHT computer team for valuable support.

[1] D. M. Basko, I. L. Aleiner, and B. L. Altshuler, Metal-insulator transition in a weakly interacting many-electron system with localized single-particle states, Ann. Phys. (N.Y.) **321**, 1126 (2006).
[2] V. Oganesyan and D. A. Huse, Localization of interacting fermions at high temperature, Phys. Rev. B **75**, 155111 (2007).
[3] R. Nandkishore and D. A. Huse, Many-body localization and thermalization in quantum statistical mechanics, Annu. Rev. Condens. Matter Phys. **6**, 15 (2015).
[4] E. Altman and R. Vosk, Universal dynamics and renormalization in many-body-localized systems, Annu. Rev. Condens. Matter Phys. **6**, 383 (2015).
[5] D. A. Abanin, E. Altman, I. Bloch, and M. Serbyn, Colloquium: Many-body localization, thermalization, and entanglement, Rev. Mod. Phys. **91**, 021001 (2019).
[6] V. Gurarie and J. T. Chalker, Some Generic Aspects of Bosonic Excitations in Disordered Systems, Phys. Rev. Lett. **89**, 136801 (2002).
[7] V. Gurarie and J. T. Chalker, Bosonic excitations in random media, Phys. Rev. B **68**, 134207 (2003).
[8] V. Gurarie, G. Refael, and J. T. Chalker, Excitations of one-dimensional Bose-Einstein condensates in a random potential, Phys. Rev. Lett. **101**, 170407 (2008).
[9] N. Bilas and N. Pavloff, Anderson localization of elementary excitations in a one-dimensional Bose-Einstein condensate, Eur. Phys. J. D **40**, 387 (2006).
[10] P. Lugan, D. Clément, P. Bouyer, A. Aspect, and L. Sanchez-Palencia, Anderson Localization of Bogolyubov Quasiparticles in Interacting Bose-Einstein Condensates, Phys. Rev. Lett. **99**, 180402 (2007).
[11] P. Lugan and L. Sanchez-Palencia, Localization of Bogoliubov quasiparticles in interacting Bose gases with correlated disorder, Phys. Rev. A **84**, 013612 (2011).
[12] S. Lellouch and L. Sanchez-Palencia, Localization transition in weakly-interacting Bose superfluids in one-dimensional quasiperdiodic lattices, Phys. Rev. A **90**, 061602(R) (2014).
[13] S. Lellouch, L.-K. Lim, and L. Sanchez-Palencia, Propagation of collective pair excitations in disordered Bose superfluids, Phys. Rev. A **92**, 043611 (2015).
[14] T. Giamarchi and H. J. Schulz, Localization and interactions in one-dimensional quantum fluids, Europhys. Lett. **3**, 1287 (1987).
[15] T. Giamarchi and H. J. Schulz, Anderson localization and interactions in one-dimensional metals, Phys. Rev. B **37**, 325 (1988).
[16] M. P. A. Fisher, P. B. Weichman, G. Grinstein, and D. S. Fisher, Boson localization and the superfluid-insulator transition, Phys. Rev. B **40**, 546 (1989).
[17] W. Krauth, N. Trivedi, and D. Ceperley, Superfluid-insulator transition in disordered boson systems, Phys. Rev. Lett. **67**, 2307 (1991).
[18] S. Rapsch, U. Schollwöck, and W. Zwerger, Density matrix renormalization group for disordered bosons in one dimension, Europhys. Lett. **46**, 559 (1999).
[19] F. D. M. Haldane, Solidification in a soluble model of bosons on a one-dimensional lattice: The Boson-Hubbard chain, J. Phys. Lett. A **80**, 281 (1980).
[20] F. D. M. Haldane, Effective Harmonic-Fluid Approach to Low-Energy Properties of One-Dimensional Quantum Fluids, Phys. Rev. Lett. **47**, 1840 (1981).
[21] M. A. Cazalilla, R. Citro, T. Giamarchi, E. Orignac, and M. Rigol, One dimensional bosons: From condensed matter systems to ultracold gases, Rev. Mod. Phys. **83**, 1405 (2011).
[22] E. Haller, R. Hart, M. J. Mark, J. G. Danzl, L. Reichsöllner, M. Gustavsson, M. Dalmonte, G. Pupillo, and H.-C. Nägerl, Pinning quantum phase transition for a Luttinger liquid of strongly interacting bosons, Nature (London) **466**, 597 (2010).
[23] G. Boéris, L. Gori, M. D. Hoogerland, A. Kumar, E. Lucioni, L. Tanzi, M. Inguscio, T. Giamarchi, C. D'Errico, G. Carleo *et al.*, Mott transition for strongly interacting one-dimensional bosons in a shallow periodic potential, Phys. Rev. A **93**, 011601(R) (2016).
[24] R. T. Scalettar, G. G. Batrouni, and G. T. Zimanyi, Localization in Interacting, Disordered, Bose Systems, Phys. Rev. Lett. **66**, 3144 (1991).
[25] P. Lugan, D. Clément, P. Bouyer, A. Aspect, M. Lewenstein, and L. Sanchez-Palencia, Ultracold Bose Gases in 1D

Disorder: From Lifshits Glass to Bose-Einstein Condensate, Phys. Rev. Lett. **98**, 170403 (2007).
[26] L. Fontanesi, M. Wouters, and V. Savona, Superfluid to Bose-Glass transition in a 1d Weakly Interacting Bose Gas, Phys. Rev. Lett. **103**, 030403 (2009).
[27] R. Vosk and E. Altman, Superfluid-insulator transition of ultracold bosons in disordered one-dimensional traps, Phys. Rev. B **85**, 024531 (2012).
[28] L. Fallani, J. E. Lye, V. Guarrera, C. Fort, and M. Inguscio, Ultracold Atoms in a Disordered Crystal of Light: Towards a Bose Glass, Phys. Rev. Lett. **98**, 130404 (2007).
[29] Y. Lahini, A. Avidan, F. Pozzi, M. Sorel, R. Morandotti, D. N. Christodoulides, and Y. Silberberg, Anderson localization and nonlinearity in one-dimensional disordered photonic lattices, Phys. Rev. Lett. **100**, 013906 (2008).
[30] M. Pasienski, D. McKay, M. White, and B. DeMarco, A disordered insulator in an optical lattice, Nat. Phys. **6**, 677 (2010).
[31] B. Deissler, M. Zaccanti, G. Roati, C. D'Errico, M. Fattori, M. Modugno, G. Modugno, and M. Inguscio, Delocalization of a disordered bosonic system by repulsive interactions, Nat. Phys. **6**, 354 (2010).
[32] B. Gadway, D. Pertot, J. Reeves, M. Vogt, and D. Schneble, Glassy Behavior in a Binary Atomic Mixture, Phys. Rev. Lett. **107**, 145306 (2011).
[33] R. Yu, L. Yin, N. S. Sullivan, J. S. Xia, C. Huan, A. Paduan-Filho, N. F. O. Jr, S. Haas, A. Steppke, C. F. Miclea *et al.*, Bose glass and Mott glass of quasiparticles in a doped quantum magnet, Nature (London) **489**, 379 (2012).
[34] C. D'Errico, E. Lucioni, L. Tanzi, L. Gori, G. Roux, I. P. McCulloch, T. Giamarchi, M. Inguscio, and G. Modugno, Observation of a Disordered Bosonic Insulator from Weak to Strong Interactions, Phys. Rev. Lett. **113**, 095301 (2014).
[35] L. Gori, T. Barthel, A. Kumar, E. Lucioni, L. Tanzi, M. Inguscio, G. Modugno, T. Giamarchi, C. D'Errico, and G. Roux, Finite-temperature effects on interacting bosonic one-dimensional systems in disordered lattices, Phys. Rev. A **93**, 033650 (2016).
[36] M. Lewenstein, A. Sanpera, V. Ahufinger, B. Damski, A. Sen, and U. Sen, Ultracold atomic gases in optical lattices: Mimicking condensed matter physics and beyond, Adv. Phys. **56**, 243 (2007).
[37] G. Modugno, Anderson localization in Bose-Einstein condensates, Rep. Prog. Phys. **73**, 102401 (2010).
[38] L. Sanchez-Palencia and M. Lewenstein, Disordered quantum gases under control, Nat. Phys. **6**, 87 (2010).
[39] Y. Lahini, R. Pugatch, F. Pozzi, M. Sorel, R. Morandotti, N. Davidson, and Y. Silberberg, Observation of a Localization Transition in Quasiperiodic Photonic Lattices, Phys. Rev. Lett. **103**, 013901 (2009).
[40] M. Verbin, O. Zilberberg, Y. Lahini, Y. E. Kraus, and Y. Silberberg, Topological pumping over a photonic Fibonacci quasicrystal, Phys. Rev. B **91**, 064201 (2015).
[41] D. Tanese, E. Gurevich, F. Baboux, T. Jacqmin, A. Lemaître, E. Galopin, I. Sagnes, A. Amo, J. Bloch, and E. Akkermans, Fractal Energy Spectrum of a Polariton Gas in a Fibonacci Quasiperiodic Potential, Phys. Rev. Lett. **112**, 146404 (2014).
[42] F. Baboux, E. Levy, A. Lemaître, C. Gómez, E. Galopin, L. Le Gratiet, I. Sagnes, A. Amo, J. Bloch, and E. Akkermans, Measuring topological invariants from generalized edge states in polaritonic quasicrystals, Phys. Rev. B **95**, 161114 (2017).
[43] B. Damski, J. Zakrzewski, L. Santos, P. Zoller, and M. Lewenstein, Atomic Bose and Anderson Glasses in Optical Lattices, Phys. Rev. Lett. **91**, 080403 (2003).
[44] R. Roth and K. Burnett, Phase diagram of bosonic atoms in two-color superlattices, Phys. Rev. A **68**, 023604 (2003).
[45] T. Roscilde, Bosons in one-dimensional incommensurate superlattices, Phys. Rev. A **77**, 063605 (2008).
[46] X. Deng, R. Citro, A. Minguzzi, and E. Orignac, Phase diagram and momentum distribution of an interacting Bose gas in a bichromatic lattice, Phys. Rev. A **78**, 013625 (2008).
[47] G. Roux, T. Barthel, I. P. McCulloch, C. Kollath, U. Schollwöck, and T. Giamarchi, Quasiperiodic Bose-Hubbard model and localization in one-dimensional cold atomic gases, Phys. Rev. A **78**, 023628 (2008).
[48] I. Bloch, J. Dalibard, and W. Zwerger, Many-body physics with ultracold gases, Rev. Mod. Phys. **80**, 885 (2008).
[49] M. Girardeau, Relationship between systems of impenetrable bosons and fermions in one dimension, J. Math. Phys. (N.Y.) **1**, 516 (1960).
[50] H. Yao, H. Khoudli, L. Bresque, and L. Sanchez-Palencia, Critical Behavior and Fractality in Shallow One-Dimensional Quasiperiodic Potentials, Phys. Rev. Lett. **123**, 070405 (2019).
[51] L. Sanchez-Palencia, Smoothing effect and delocalization of interacting Bose-Einstein condensates in random potentials, Phys. Rev. A **74**, 053625 (2006).
[52] See Supplemental Material at http://link.aps.org/supplemental/10.1103/PhysRevLett.125.060401 for a discussion on single-particle localization, fractal properties, and details for QMC calculations, which includes Refs. [23,34,50,53–59].
[53] J. Biddle, B. Wang, D. J. Priour Jr, and S. Das Sarma, Localization in one-dimensional incommensurate lattices beyond the Aubry-André model, Phys. Rev. A **80**, 021603 (2009).
[54] F. Meinert, M. Panfil, M. J. Mark, K. Lauber, J.-S. Caux, and H.-C. Nägerl, Probing the Excitations of a Lieb-Liniger Gas from Weak to Strong Coupling, Phys. Rev. Lett. **115**, 085301 (2015).
[55] M. Boninsegni, N. Prokof'ev, and B. Svistunov, Worm Algorithm for Continuous-Space Path Integral Monte Carlo Simulations, Phys. Rev. Lett. **96**, 070601 (2006).
[56] M. Boninsegni, N. V. Prokof'ev, and B. V. Svistunov, Worm algorithm and diagrammatic Monte Carlo: A new approach to continuous- space path integral Monte Carlo simulations, Phys. Rev. E **74**, 036701 (2006).
[57] D. M. Ceperley, Path integrals in the theory of condensed helium, Rev. Mod. Phys. **67**, 279 (1995).
[58] G. Carleo, G. Boéris, M. Holzmann, and L. Sanchez-Palencia, Universal Superfluid Transition and Transport Properties of Two-Dimensional Dirty Bosons, Phys. Rev. Lett. **111**, 050406 (2013).
[59] H. Yao, D. Clément, A. Minguzzi, P. Vignolo, and L. Sanchez-Palencia, Tan's contact for trapped Lieb-Liniger bosons at finite temperature, Phys. Rev. Lett. **121**, 220402 (2018).
[60] M. Olshanii, Atomic Scattering in the Presence of an External Confinement and a Gas of Impenetrable Bosons, Phys. Rev. Lett. **81**, 938 (1998).

[61] For the finite system size $L = 83a$, the ratio $r \simeq 0.807 \simeq 67/83$ is a fair approximation for an irrational number since no periodicity is realized.

[62] J. Biddle and S. Das Sarma, Predicted mobility edges in one-dimensional incommensurate optical lattices: An exactly solvable model of Anderson localization, Phys. Rev. Lett. **104**, 070601 (2010).

[63] A. Szabó and U. Schneider, Non-power-law universality in one-dimensional quasicrystals, Phys. Rev. B **98**, 134201 (2018).

[64] F. Gerbier, Boson Mott Insulators at Finite Temperatures, Phys. Rev. Lett. **99**, 120405 (2007).

[65] The gap of the smallest lobes does not vary much with the interaction strength while that of the largest lobes does; see Fig. 1. It explains that only $T_2^\star$ varies significantly with the interaction strength in Fig. 3.

[66] T. P. Meyrath, F. Schreck, J. L. Hanssen, C.-S. Chuu, and M. G. Raizen, Bose-Einstein condensate in a box, Phys. Rev. A **71**, 041604 (2005).

[67] A. L. Gaunt, T. F. Schmidutz, I. Gotlibovych, R. P. Smith, and Z. Hadzibabic, Bose-Einstein Condensation of Atoms in a Uniform Potential, Phys. Rev. Lett. **110**, 200406 (2013).

[68] L. Chomaz, L. Corman, T. Bienaimé, R. Desbuquois, C. Weitenberg, S. Nascimbène, J. Beugnon, and J. Dalibard, Emergence of coherence via transverse condensation in a uniform quasi-two-dimensional Bose gas, Nat. Commun. **6**, 6162 (2015).

[69] J. Vidal, D. Mouhanna, and T. Giamarchi, Correlated Fermions in a One-Dimensional Quasiperiodic Potential, Phys. Rev. Lett. **83**, 3908 (1999).

[70] J. Vidal, D. Mouhanna, and T. Giamarchi, Interacting fermions in self-similar potentials, Phys. Rev. B **65**, 014201 (2001).

[71] M. Troyer, B. Ammon, and E. Heeb, Parallel object oriented Monte Carlo simulations, Lect. Notes Comput. Sci. **1505**, 191 (1998).

[72] A. Albuquerque, F. Alet, P. Corboz, P. Dayal, A. Feiguin, S. Fuchs, L. Gamper, E. Gull, S. Guertler, A. Honecker *et al.*, The ALPS project release 1.3: Open-source software for strongly correlated systems, J. Magn. Magn. Mater. **310**, 1187 (2007).

[73] B. Bauer, L. D. Carr, H. Evertz, A. Feiguin, J. Freire, S. Fuchs, L. Gamper, J. Gukelberger, E. Gull, S. Guertler *et al.*, The ALPS project release 2.0: Open source software for strongly correlated systems, J. Stat. Mech. (2011) P05001.